

## OPTIMIZATION OF ORGAN FREEZING PROTOCOLS WITH SPECIFIED ALLOWABLE THERMAL STRESS LEVELS

Brian H. Dennis<sup>1</sup> and George S. Dulikravich<sup>2</sup>

Multidisciplinary Analysis, Inverse Design, and Optimization (MAIDO) Program  
Department of Mechanical and Aerospace Engineering, UTA Box 19018  
The University of Texas at Arlington, Arlington, TX 76019-0018, U.S.A.  
Phone: +1 (817) 272-7376 FAX: +1 (817) 272-5010 E-mail: gsd@mae.uta.edu

Yoed Rabin<sup>3</sup>

Department of Mechanical Engineering, Carnegie Mellon University  
5000 Forbes Avenue, Pittsburgh, PA 15213  
Phone: +1 (412) 268-2204 Fax: +1 (412) 268-3348 E-mail: rabin@cmu.edu

### ABSTRACT

A novel concept of determining optimized cooling protocols for freezing three-dimensional organs has been developed and its feasibility examined computationally. The concept is based on determining correct spatial variation of temperature distribution on the walls of a freezing container at every instant of time during the cooling process so that local thermal stresses in the heterogeneous organ are always kept below a specified level while maximizing the local cooling rates. The cryo-preservation medium must be gelatin which prevents thermal convection. The optimized cooling protocol was simulated by developing a time-accurate finite element computer program to predict unsteady heat conduction with phase change and thermal stresses within a realistically shaped and sized organ made of tissues with temperature-dependent physical properties. A micro-genetic optimization algorithm was then used to achieve nonlinear constrained optimization of parameterized time-varying container wall temperature distribution so that the prescribed maximum allowable thermal stresses are never exceeded in the organ.

### NOMENCLATURE

C = specific heat per unit mass  
E = Young's modulus of elasticity  
F = fitness function in the optimization  
G = shear modulus  
H = latent heat per unit mass  
k = thermal conductivity coefficient  
t = time  
P = penalty term in the optimization  
T = temperature  
u = deformation in x-direction  
v = deformation in y-direction  
z = deformation in z-direction  
x,y,z = Cartesian coordinate directions

### Greek Letters

$\alpha$  = thermal diffusion coefficient  
 $\beta$  = thermal expansion coefficient  
= Poisson's ratio  
 $\sigma$  = stress  
 $\rho$  = density

### INTRODUCTION

Shortage of available human organs is the most serious problem encountered by patients in need of organ transplantation. Using current organ preservation protocols

<sup>1</sup> Graduate research assistant. Student member ASME.

<sup>2</sup> Professor. Fellow ASME.

<sup>3</sup> Associate Professor.

which have the organ packed in ice at 4 degrees Celsius with a solution called UW (for University of Wisconsin) that is a mix of electrolytes, organs have the following average shelf lives from harvest to implantation: heart 4 - 6 hours, lungs 4 - 6 hours, kidney 24 - 48 hours, and liver 36 - 48 hours. A possible solution would be to completely freeze the organs and establish an organ bank that could store organs with different immunological properties in a frozen state for lengthy periods of time.

During the past three decades there have been numerous attempts at freezing the organs. When preserving living human organs (kidney, heart, lungs, spleen, liver, bone, etc.) for the purpose of performing transplant surgery, the organ is typically cooled in a special cryo-protective agent (CPA) liquid while perfused by a cooling CPA liquid to a prescribed subfreezing temperature. If the cooling rate is too high, strong residual thermal stresses will cause fractures in the frozen tissues (Rabin et al., 1997). If the cooling rate is too slow, chemical decomposition and dehydration in the tissue will make the organ useless (Mazur, 1970). Experiments have shown that although a whole organ does not survive freezing, cells and smaller parts of the organ often survive (Jacobsen and Pegg, 1984; Hayes et al., 1987; Jacobsen et al., 1984). Thus, there has been a common belief that there is an optimal cooling rate for each particular type of tissue of an organ in order to maximize the survivability of the living cells and reduce the problem of future rejection by the organ recipient's body.

Most of the attempts to develop controlled rate cooling devices (Kelley et al., 1982) employ either a liquid cooling bath with ethanol or liquid nitrogen as the heat-exchange medium or a cooling chamber with vaporized liquid nitrogen as the coolant. In both cases the heat transfer from the organ to the CPA and from the CPA to the freezing container is by convection thus creating almost uniform surface temperature on both organ and the container. Consequently, an almost uniform cooling rate is achieved during such convective cooling at every point on the outside surface of the organ. Although this surface cooling rate can be kept at some optimum level (Fahy, 1981), numerical analysis of organ freezing has shown that thermal boundary conditions are not propagated uniformly into the interior, resulting in a non-uniform distribution of temperature histories and cooling rates throughout the spatial domain (Hayes et al., 1984). Thus, this standard cooling protocol results in considerably different values of local cooling rates inside the organ and consequently create extreme values of residual thermal stresses in the organ which cause organ fractures.

One concept that offers a possible practical solution to freezing and thawing of organs is to immerse them in a gelatin CPA thus assuring that the heat transfer from the outer surface of the organ to such CPA will occur by pure conduction. A plausible objective is then to find the proper time variation of surface thermal conditions of the freezing container wall so that the optimal local cooling rates are achieved at each instant of time at every point inside the organ. This concept was demonstrated as numerically

feasible in a two-dimensional approximation without phase change (Madison et al., 1987; Dulikravich, 1988; Dulikravich and Hayes, 1988; Dulikravich et al., 1989; Ambrose et al., 1989). However, it has been impossible to preserve large organs even when the local cooling rates are apparently identical to those proven successful for small samples from the organ (Jacobsen and Pegg, 1984), because of the fractures caused by the thermal stresses.

Thus, the objective during the freezing or thawing should not be to enforce experimentally obtained local optimal cooling rates since they apply to small tissue samples rather than whole organs. One of the main objectives should be to limit the thermal stresses that cause the fractures in the organs (Rabin and Steif, 1998; 2000; Rabin et al., 1996; 1997; 1998) while minimizing the overall freezing time. Other significant damaging mechanisms are ice crystal formation, blood vessel deterioration, cell dehydration, and the toxicity effect of the CPA (Fahy, 1981; Guttman et al., 1986).

The basic proof-of-the-concept paper (Dennis and Dulikravich, 2000) did not fully account for different tissues in a realistic organ, it did not account for temperature-dependent thermal properties, and did not utilize a refined computational grid. This paper accounts for these features, but still does not account for thermal stresses due to phase change.

## MATHEMATICAL MODEL

It is a well-known fact that tissues and organs are characterized by non-isotropic mechanical and thermal properties. Since these properties are not well documented in the open literature, in this work we will assume that the Navier equations for linear unsteady deformations  $u, v, w$  in three-dimensional Cartesian  $x, y, z$  coordinates are valid. Inertia terms are expected to be negligible during the freezing or thawing processes. Thermoelasticity field is then governed by the following system of differential equations.

$$(\lambda + G) \left( \frac{\partial^2 u}{\partial x^2} + \frac{\partial^2 v}{\partial x \partial y} + \frac{\partial^2 w}{\partial x \partial z} \right) + G \nabla^2 u + X = 0 \quad (1)$$

$$(\lambda + G) \left( \frac{\partial^2 u}{\partial x \partial y} + \frac{\partial^2 v}{\partial y^2} + \frac{\partial^2 w}{\partial y \partial z} \right) + G \nabla^2 v + Y = 0 \quad (2)$$

$$(\lambda + G) \left( \frac{\partial^2 u}{\partial x \partial z} + \frac{\partial^2 v}{\partial y \partial z} + \frac{\partial^2 w}{\partial z^2} \right) + G \nabla^2 w + Z = 0 \quad (3)$$

$$\lambda = \frac{Ev}{(1+\nu)(1-2\nu)}, \quad G = \frac{E}{2(1+\nu)} \quad (4)$$

The body forces per unit volume due to stresses caused by thermal expansion/contraction over the temperature range  $\Delta T$  are

$$X = -(3\lambda + 2G) \frac{\partial(\beta \Delta T)}{\partial x} \quad (5)$$

$$Y = -(3\lambda + 2G) \frac{\partial(\beta \Delta T)}{\partial y} \quad (6)$$

$$Z = -(3\lambda + 2G) \frac{\partial(\beta\Delta T)}{\partial z} \quad (7)$$

The linear thermoelasticity system also includes unsteady energy conservation equation with latent heat of liquid/solid phase change lumped together with specific heat, that is,

$$\frac{\partial(\rho C_{\text{effective}} T)}{\partial t} = \nabla \cdot (k \nabla T) \quad (8)$$

The effective specific heat is a combination of the actual specific heat and the temperature variation of the latent heat,  $L$ , incorporated in the volumetric enthalpy,  $H$ , so that

$$\rho C_{\text{effective}} = \frac{\partial H}{\partial T} = \left( \frac{\nabla H \cdot \nabla H}{\nabla T \cdot \nabla T} \right)^{1/2} \quad (9)$$

All physical properties in this model are allowed to vary as function of space and temperature. The latent heat was applied only in the mushy region, that is, at the points where the local instantaneous predicted temperature was between liquidus and solidus values.

## PHYSICAL PROPERTIES

Because of its relatively simple and compact geometry and the relative wealth of published experimentally measured therophysical properties (Hayes, 1981; Bowman et al., 1975; Rabin et al., 1996), we have chosen a dog kidney as an example realistic three-dimensional organ to simulate the new concept of optimized freezing protocol.

Although the actual kidney is composed of many distinctive tissues, we will restrict this model to only four major tissue domains: cortex (the most outer layer), medulla (the congruent inner layer), pelvis (the central domain), and fat (the domain that connects the pelvis with a part of the concave portion of the kidney surface).

Measured values of physical properties available in the open literature vary significantly. Consequently, we used the

values that for the most part represent the average values. In the case of the gelatin CPA we used thermophysical properties of a low concentration gelatin, just at the level that prevents heat convection by thermal buoyancy (about 1.3 percent by weight). In this case, gelatin behaves similarly to water and ice.

## DISCRETIZATION AND PARAMETERIZATION

Due to its simple shape and the relative availability of thermophysical data, we chose to demonstrate this optimized freezing protocol concept on an example of a dog kidney. The two inner regions of the kidney (fat and pelvis), kidney intermediate congruent region (medulla), and kidney outer region (cortex), and the spherical container shapes were created by generating four concentric cubes. Each of the six faces of each of the four cubes was discretized with a structured grid of quadrilateral cells. The four concentric cubes were then transformed into four concentric spheres by dividing  $x, y, z$  coordinates of every grid point on every original cube with the radial distance of the corresponding point on the most outer cube. The six faces of the most outer cube then became the six deformed quadrilateral patches making up the surface of the spherical freezing container. The kidney cortex and the imbedded medulla and pelvis spherical shapes were then analytically transformed into concentric ellipsoids that were consequently analytically bent. The fat tissue region was created as a non-congruent part of the pelvis domain. The surface grids consisting of deformed quadrilaterals (Fig. 1) were then connected with quasi-radial lines thus creating a fully boundary conforming three-dimensional structured grid permeating the entire organ and the surrounding gelatin.

The surface variation of temperature on the spherical container wall was parameterized with biquadratic Lagrange polynomials using 9 control points for each of the large six deformed quadrilateral patches forming the container wall thus resulting in a total of 26 design variables (container wall temperatures) that will need to be determined at each instant during the cooling process.

Table 1. Thermal properties of dog kidney tissues and the gelatin (unfrozen) (Valvano et al., 1985)

|         | Heat capacity per unit volume:<br>$\rho C = (k0/\alpha0) + (k1/\alpha0) T$<br>[J m <sup>-3</sup> C <sup>-1</sup> ] |                          | Latent heat per unit volume: $\rho H$<br>[MJ m <sup>-3</sup> ] | Thermal conductivity<br>$k = k0 + k1 T$ (T in C)<br>[W m <sup>-1</sup> C <sup>-1</sup> ] |           | Thermal diffusivity<br>$\alpha = 10^6 (\alpha0 + \alpha1 T)$ (T in C)<br>[m <sup>2</sup> s <sup>-1</sup> ] |          |
|---------|--|--------------------------|--|--|-----------|--|----------|
|         | k0   | k1                       |  | $\alpha0$  | $\alpha1$ |  |          |
| Gelatin | 4.19 x 10 <sup>6</sup>   |                          | 330.0  | 0.595  |           | 0.142  |          |
| Cortex  | 3.68 x 10 <sup>6</sup>   | 9.602 x 10 <sup>3</sup>  | 250.0  | 0.4905   | 0.001280  | 0.1333   | 0.00039  |
| Medulla | 3.88 x 10 <sup>6</sup>   | 9.946 x 10 <sup>3</sup>  | 240.0  | 0.5065   | 0.001298  | 0.1305   | 0.00063  |
| Pelvis  | 3.695 x 10 <sup>6</sup>  | 7.908 x 10 <sup>3</sup>  | 225.0  | 0.4930   | 0.001055  | 0.1334   | 0.00052  |
| Fat     | 2.597 x 10 <sup>6</sup>  | -1.922 x 10 <sup>3</sup> | 66.7   | 0.3431   | -0.000254 | 0.1321   | -0.00002 |

Table 2. Thermal properties of dog kidney tissues and the gelatin (frozen)

| Symbols & Units   | Average for Kidney Tissues   | Gelatin                           | Source             |
|---|--|-----------------------------------|--------------------|
| temperature (liquidus): $T_l$ [C]   | 0.0  | 0.0                               | assumed            |
| temperature (solidus): $T_s$ [C]  | -22.0  | -3.0                              | assumed            |
| heat capacity per unit volume (frozen): $\rho C_s$ [J m <sup>-3</sup> K <sup>-1</sup> ] | $1.8 \times 10^6$ (value at 265 K)   | $113 \times 10^6$                 | Rabin et al., 1996 |
| thermal conductivity (frozen): $k_s$ [W m <sup>-1</sup> K <sup>-1</sup> ]               | $1967.0 \times T^{-1.235}$ (T<265 K)<br>$2.0 - (T - 265.0) \times 0.0595$<br>(265 K < T < 273 K) | $2135 \times T^{-1.235}$          | Rabin, 2000        |
| thermal diffusivity: (frozen): $\alpha_s$ [m <sup>2</sup> s <sup>-1</sup> ]             | $1.0 \times 10^{-6}$   | $1.986 \times 10^{-6}$            | Rubinsky, 1989     |
| volumetric thermal expansion (frozen): $\beta_s$ [K <sup>-1</sup> ]                     | $(0.29 T - 14.0) \times 10^{-6}$   | $(0.25 T - 12.25) \times 10^{-6}$ | Rabin et al., 1998 |
| Young's modulus of elasticity (unfrozen): $E$ [N m <sup>-2</sup> ]                      | $22.9 \times 10^6$   | $10.0 \times 10^6$                | assumed            |
| Young's modulus of elasticity (frozen): $E_s$ [N m <sup>-2</sup> ]                      | $22.9 \times 10^9$   | $10.0 \times 10^9$                | Rabin et al., 1996 |
| Poisson's ratio (unfrozen): $\nu$   | 0.333  | 0.333                             | assumed            |
| Poisson's ratio (frozen): $\nu_s$   | 0.333  | 0.333                             | assumed            |
| yield stress (frozen): $\sigma_Y$ [N m <sup>-2</sup> ]                                  | $100.0 \times 10^6$  | $10.0 \times 10^6$                | Rabin et al., 1996 |
| maximum allowed stress (frozen): $\sigma_{allow}$ [N m <sup>-2</sup> ]                  | $66.0 \times 10^6$   | N/A                               | Rabin et al., 1996 |
| maximum stress (frozen): $\sigma_{max}$ [N m <sup>-2</sup> ]                            | $132.2 \times 10^6$  | N/A                               | Rabin et al., 1996 |

## OPTIMIZATION

Then, the transient temperature distribution was computed at every point of the organ using our three-dimensional linear thermoelasticity finite element method analysis code subject to initially guessed 26 values for the local wall temperature on the spherical container surface. From this, the actual local temperature gradients and thermal stresses were determined at each point in the organ. A nonlinear constrained function maximization method based on a genetic algorithm (Dennis et al., 1999; Dulikravich et al., 1999) was used after certain time interval,  $\Delta t$ , to optimize the 26 values of temperature at each of the control points on the spherical container surface. That is, the new temperature distribution on the container walls was determined so that it maximizes the average cooling rate in the organ for the given time interval while keeping the local thermal stresses in the organ below a user specified maximum allowable value. The algorithm is outlined in Figure 2. The fitness function,  $F$ , that was maximized every time interval,  $\Delta t$ , was

$$F = - \left[ \frac{\Delta T}{\Delta t} + P \left( \frac{\sigma_{max}}{\sigma_Y} \right)^2 \right] \quad (10)$$

where  $\Delta T = T_{final} - T_{initial}$  and  $\Delta t = t_{final} - t_{initial}$  and  $P$  is a user specified penalty term. Notice that the cooling rate is a negative number.

## NUMERICAL RESULTS

The system of equations (1-3) and (8) was integrated numerically using a finite element method on a tetrahedral non-structured grid, ILU and preconditioned Krylov subspace methods, and object-oriented programming in C++ (Dennis and Dulikravich, 1999). The accuracy of the finite element code for heat conduction involving solidification was verified through comparison with a known analytic solution. The solidification of a liquid rod, which has an analytic solution, was simulated using a 3-D mesh of a rod composed of 480 parabolic tetrahedral elements. Figure 3 shows the variation of temperature with time for a specific point on the rod for both analytic and numerical solutions. The temperature was taken over a given time interval at a specific internal point inside the mesh. The numerical solution, though quite accurate is not exactly the same as the analytic solution. In our FEM

implementation of the phase change, the temperature interval during which phase changes must be larger than zero. For calculating the rod case, a temperature interval of 1°C was used. However, the analytic solution corresponds to phase change of a pure substance for which this temperature interval is zero. This non-zero temperature interval in the FEM model is the most likely source of the slight discrepancy between the numerical and the analytic results. A very small temperature interval for the phase change can be used. However, in this case it was found that an unreasonably small time step was required to obtain solutions with an almost perfect agreement with the analytic solution.

The three-dimensional freezing protocol simulation and optimization algorithm was then applied to a geometry composed of five domains. The outer boundary was a spherical freezing container. Within the container was gelatin and a kidney consisting of a cortex, medulla, pelvis, and fat (Fig. 1). The optimizer was applied after every  $\Delta t = 10$  minutes. The penalty term in the objective function,  $P$ , was fixed at  $P = 100$  when the maximum von Mises stress in the kidney domain,  $\sigma_{\max}$ , was greater than the local yield stress,  $\sigma_{\text{yield}}$ . The penalty term was  $P = 0$  for all other situations. The genetic algorithm (GA) used 4 bit strings to represent each of the 26 design variables (container surface node temperatures). Each of these variables was allowed to vary from 20°C to -100°C. A uniform crossover operator was used with a 50% chance of crossover. A fixed population size of 31 was used with a 2% chance of mutation. Each optimization cycle was run for 30 generations and was executed on our distributed memory parallel computer made of 32 Intel 400MHz processors running MPI. Each analysis run, which was composed of simulation of three-dimensional heat conduction with a moving freezing front in this multi-domain region including thermal stress analysis, required 5 minutes on a single CPU. Eight node trilinear hexahedral elements were used for heat conduction and stress analysis. A total of 5832 elements were used. A time step of 60 seconds was used for each transient heat conduction analysis.

Figure 4 shows the computed variation of the maximum temperature with time for each of the four kidney tissue domains. It appears that the cooling rate (based on maximum temperature variation) in each of the four tissues should increase with time. In this test case it took 36 minutes before the cooling front arrived from the container surface to the kidney surface. This time can be significantly reduced by using thinner region of the gelatin, and by using gelatins with higher thermal diffusivity. Figure 5 shows the computed temperature distribution for different times along the long axis of the kidney. Notice that after 158 minutes, the kidney has been completely frozen. The temperature distribution should be symmetric since both the geometry and the initial thermal conditions are symmetric. The occasional asymmetry is most likely due to incomplete convergence of the GA algorithm since each of the 26 nodal temperatures on the container surface is allowed to vary in a wide range between +20.0 and -100.0 degrees

Celsius. Figure 5 can also serve to demonstrate that the optimum cooling rates should not have fixed values, but must vary in space and time to keep the three-dimensional thermal stresses below a specified value during the freezing process.

Figure 6 shows time evolution of the computed maximum stress in each kidney domain for each of the optimized container surface temperature distributions. Figure 8 depicts time evolution of von Mises stresses computed along the long axis of the kidney. Figure 9 shows Von Mises stresses predicted on the x-y plane at  $z = 0$  after 9140 seconds. The noticeable local errors in the computed results are due to a poor quality grid (Figure 10). It is interesting that at some locations on the container surface the optimizer found that temperatures should temporarily increase after some time intervals (Figs. 11-13). This is caused by the imposed constraint on the maximum allowable local thermal stresses.

## CONCLUSIONS

In this substantiated proof of concept study it has been successfully demonstrated that it is possible to numerically simulate the entire freezing protocol of realistic three-dimensional organs. Moreover, it has been successfully demonstrated numerically that it is possible to control the damage caused by the thermal stresses during freezing of organs by periodically optimizing temperature distribution on the surface of the freezing container. Using more diverse tissue sub-domains, more accurate non-isotropic thermophysical data, finer spatial and temporal discretization, and more geometrically complicated configurations of organs and containers is a relatively straightforward future extension of this work. However, a considerably more challenging extension of this work would be to incorporate thermal stresses due to phase change and optimally controlled unsteady internal perfusion of the organ during the freezing.

## LITERATURE

Ambrose, C., Hayes, L. J., and Dulikravich, G. S. (1989). "An Active Control System for Thermal Fields in Hypothermic Processes," ASME National Heat Transfer Conference, Philadelphia, PA, Aug. 6-9, 1989, eds: S. B. Yilmaz, *AICHE Symposium Series 269*, Vol. 85, pp. 440-405.

Bowman, H. F., Cravalho, E. G. and Woods, M., (1975) "Theory, Measurement, and Application of Thermal Properties of Biomaterials," *Annual Review of Biophysics and Bioeng.*, Vol. 4, pp. 43-80.

Dennis, B. H. and Dulikravich, G. S., (1999) "Simultaneous Determination of Temperatures, Heat Fluxes, Deformations, and Tractions on Inaccessible Boundaries," *ASME Journal of Heat Transfer*, Vol. 121, pp. 537-545.

Dennis, B. H., and Dulikravich, G. S., (2000) "Determination of Unsteady Container Temperatures During Freezing of Three-dimensional Organs With Constrained Thermal Stresses," *Internat. Symposium on Inverse Problems*

in *Engineering Mechanics – ISIP'2k*, (eds: M. Tanaka and G. S. Dulikravich), Nagano, Japan, March 7-10, 2000, Elsevier.

Dennis, B. H., Dulikravich, G. S. and Han, Z.-X., (1999) "Constrained Optimization of Turbomachinery Airfoil Cascade Shapes Using a Navier-Stokes Solver and a Genetic/SQP Algorithm," ASME paper 99-GT-441, ASME Turbo Expo, Indianapolis, IN, June 7-10, 1999.

Dulikravich, G. S., (June 1988) "Inverse Design and Active Control Concepts in Strong Unsteady Heat Conduction," *Appl. Mech. Rev.*, Vol. 41, No. 6, pp. 270-277.

Dulikravich, G. S. and Hayes, L. J., (1988) "Control of Surface Temperatures to Optimize Survival in Cryopreservation," ASME Winter Annual Meeting, Chicago, Illinois, Nov. 27 - Dec.2, 1988, *Proceedings of the Symposium on Computational Methods in Bioengineering*, (eds: Spilker, R. L. and Simon, B. R.), ASME BED-Vol. 9, pp. 255-265.

Dulikravich, G. S., Madison, J. V., and Hayes, L. J., (1989) "Control of Interior Cooling Rates in Heterogeneous Materials by Varying, Surface Thermal Boundary Conditions," 1st Pan-American Congress of Applied Mechanics (PACAM), eds: C. R. Steele and L. Bevilacqua, Rio de Janeiro, Brazil, January 3-6, 1989, pp. 420-423.

Dulikravich, G. S., Martin, T. J., Dennis, B. H. and Foster, N. F., (1999) "Multidisciplinary Hybrid Constrained GA Optimization," *EUROGEN'99 - Evolutionary Algorithms in Engineering and Computer Science: Recent Advances and Industrial Applications*, (eds: K. Miettinen, M. M. Makela, P. Neittaanmaki and J. Periaux), John Wiley & Sons, Ltd., Jyväskylä, Finland, May 30 - June 3, 1999.

Fahy, G. M., (1981) "Analysis of "Solution Effects" Injury: Cooling Rate Dependence of the Functional and Morphological Sequellae of Freezing in Rabbit Renal Cortex Protected with Dimethyl Sulfoxide," *Cryobiology*, Vol. 18, pp. 550-570.

Guttman, F. M., Milhomme, G., Gibbons, L. and Seemayer, T. A., (1986) "Variation of Cooling Rate and Concentration of Dimethyl Sulfoxide on Rabbit Kidney Function," *Cryobiology*, Vol. 23, pp. 495-499.

Hayes, L. J., (1981) "Experimental Values of Tissue-Dependent Thermal Properties of the Kidney," TICOM Report 81-8, University of Texas, Austin, TX.

Hayes, L. J., Diller, K. R., Lee, H. S. and Baxter, C. R., (1984) "On the Definition of an Average Cooling Rate During Cell Freezing," *Cryo-Letters*, Vol. 5, pp. 97-110.

Hayes, L. J., Diller, K. R. and Lee, H. S., (1987) "Prediction of Local Cell Survival in Cryopreservation of Large Specimens," *Cryobiology*, Vol. 25, pp. 101-121.

Jacobsen, I. A., Pegg, D. E., Starklint, H., Chemnitz, J., Hunt, C., Barfort, P. and Diaper, M. P., (1984) "Effect of Cooling and Warming Rate on Glycerolized Rabbit Kidneys," *Cryobiology*, Vol. 21, pp. 637-653.

Jacobsen, I. A. and Pegg, D. E., (1984) "Cryopreservation of Organs: A Review," *Cryobiology*, Vol. 21, pp. 377-384.

Kelley, F. D., Phelan, R. M. and Levin, R. L., (1982) "Controlled-Rate Liquid N-Microwave Biological Freeze-Thaw Device," *Cryobiology*, Vol. 19, pp. 372-391.

Madison, J. V., Dulikravich, G. S., and Hayes, L. J., (1987) "Optimization of Container Wall Temperature Variation During Transplant Tissue Cooling," International Conference on Inverse Design Concepts and Optimization in Eng. Sciences (ICIDES-II), eds: G. S. Dulikravich, Penn State University, University Park, PA, Oct. 26-28, 1987, pp. 321-336.

Mazur, P., (1970) "Cryobiology: The freezing of Biological Systems," *Science*, Vol. 168, pp. 939-949.

Rabin, Y., (2000) "The Effect of Temperature-Dependent Thermophysical Properties in Heat Transfer Simulations of Biomaterials in Cryogenic Temperatures", *Cryo-Letters*, Vol. 21, No. 3, pp. 163-170.

Rabin, Y., Olson, P., Taylor, M. J., Steif, P. S., Julian, T. B., and Wolmark, N., (1997) "Gross Damage Accumulation in Frozen Rabbit Liver Due to Mechanical Stress at Cryogenic Temperatures," *Cryobiology*, Vol. 34, pp. 394-405.

Rabin, Y., Taylor, M. J., and Wolmark, N., (1998) "Thermal Expansion Measurements of Frozen Biological Tissues at Cryogenic Temperatures," *ASME J. of Biomech. Eng.*, Vol. 120, No. 2, pp. 259-266.

Rabin, Y., and Steif, P. S., (1998) "Thermal Stresses in a Freezing Sphere and its Application to Cryobiology," *ASME J. of Applied Mechanics*, Vol. 65, No. 2, pp. 328-333.

Rabin, Y., and Steif, P. S., (2000) "Thermal Stress Modeling in Cryosurgery," *Int. J. of Solids and Structures*, Vol. 37, pp. 2363-2375

Rabin, Y., Steif, P. S., Taylor, M. J., Julian, T. B., and Wolmark, N., (1996) "An Experimental Study of the Mechanical Response of Frozen Biological Tissues at Cryogenic Temperatures," *Cryobiology*, Vol. 33, pp. 472-482.

Rubinsky, B., (August 1986) "Recent Advances in Cryopreservation of Biological Organs and in Cryosurgery," *Proc. of 8th Internat. Heat Transfer Conf.*, San Francisco, CA.

Valvano, J. W., Cochran, J. R., and Diller, K. R., (May 1985) "Thermal Conductivity and Diffusivity of Biomaterials Measured with Self-Heated Thermistors," *International Journal of Thermophysics*, Vol. 6, No. 3, pp. 301-310.

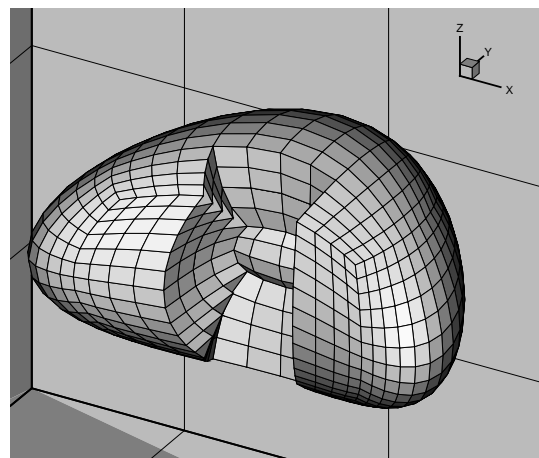


Figure 1. Kidney geometry with fat region removed.

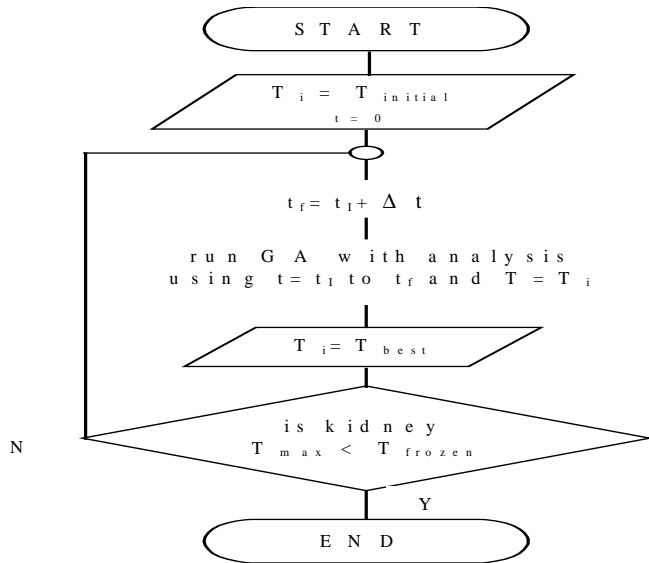


Figure 2. Algorithm for inverse determination of unsteady thermal boundary conditions on the freezing container surface.

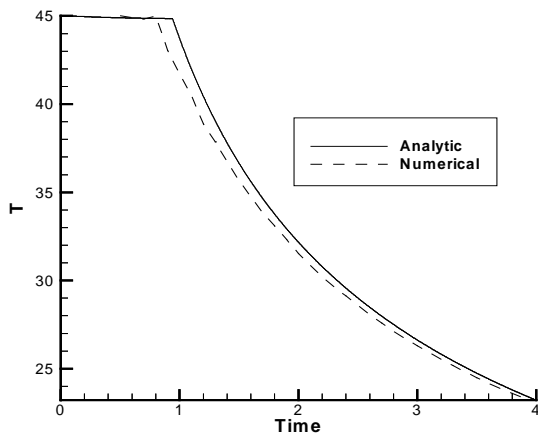


Figure 3. Comparison of analytic and numerical solution for the freezing of a 1-D slab at  $x=1$ .

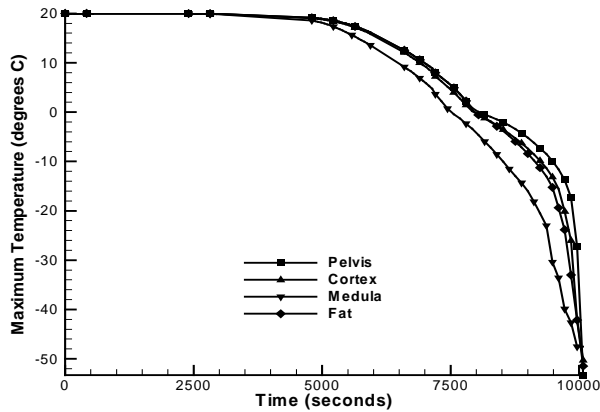


Figure 4. Variation of maximum temperature with time in each kidney region for optimized container temperature distributions.

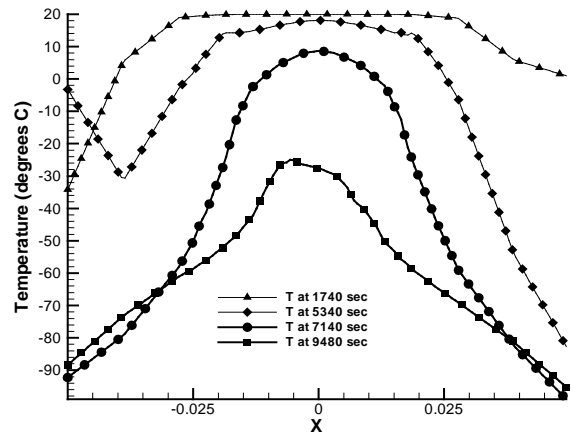


Figure 5. Variation of internal temperature distribution in time along line of intersection between  $x-z$  plane at  $y = 0$  and  $x-y$  plane at  $z = 0$  (see Figure 1).

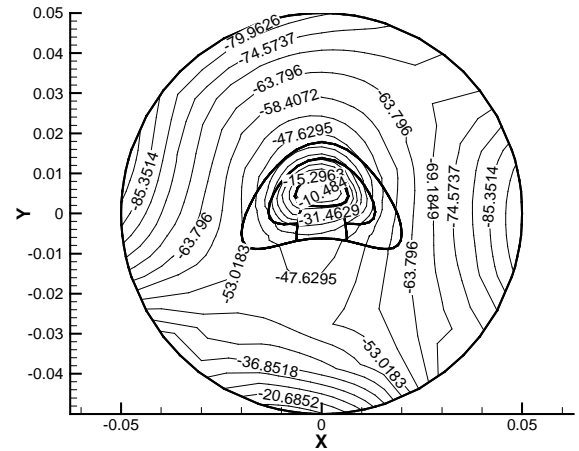


Figure 6. Isotherms on the  $x-y$  plane at  $z = 0$  after two hours and 38 minutes using periodic optimization of container surface temperature distribution.

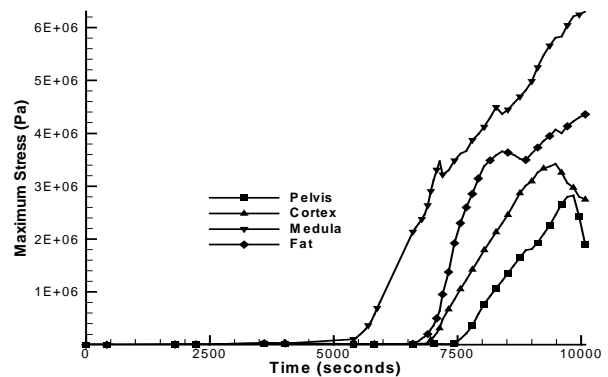


Figure 7. Variation of maximum stress with time in each kidney region for optimized container temperature distributions.

